Journal of The Electrochemical Society, **153** (11) A2139-A2146 (2006)
0013-4651/2006/153(11)/A2139/8/$20.00 © The Electrochemical Society

Dynamics of Autohumidifed PEM Fuel Cell Operation

Warren H. J. Hogarth[a,b] **and Jay B. Benziger**[a,z]

[a]*Department of Chemical Engineering, Princeton University, Princeton, New Jersey 08544, USA*
[b]*ARC Centre for Functional Nanomaterials, The University of Queensland, Brisbane, QLD 4072 Australia*

Start-up and dynamic responses to changes in load are reported for a dry feed, autohumidified polymer electrolyte membrane fuel cell (PEMFC). The fuel cell current can be ignited by water injection; criteria are derived for the required water injection as functions of fuel cell size, temperature, and reactant feed rates. Steady-state multiplicity is observed where the fuel cell current can be either high ("ignited") or low ("extinguished") with the same flow rates, temperature, pressure, and load. Different steady-state voltages were obtained for the same current depending on the operational history. The steady-state multiplicity results from a positive feedback between the membrane resistance and water production. Membrane water content is determined from the balance of water produced and water removed by convection. Current ignition occurs when the water produced is greater than its removal, hydrating the membrane; current extinction occurs when the water produced is less than its removal, which dehydrates the membrane. Through the use of mass balances and constitutive equations, design criteria are obtained for sizing and operating autohumidified PEMFCs.
 [DOI: 10.1149/1.2344841]

Manuscript submitted March 1, 2006; revised manuscript received June 13, 2006. Available electronically September 15, 2006.

Polymer electrolyte membrane fuel cells (PEMFCs) are well suited for intermittent power generation because they function at mild conditions from 0 to 100°C, 1–3 bar pressure, and are relatively simple to maintain. The current state of the art PEMs must be hydrated to provide adequate proton conductivity. Consequently, these systems have employed humidified feed streams which require the inclusion of humidifier systems that can operate over a range of temperatures. The humidification systems add weight and complexity to the overall fuel cell system. Major fuel cell developers including Ballard[1] and GM[2] have identified the need for a reduction in system complexity and removal of the need to humidify gas streams as important steps to achieve fuel cell commercialization.

Autohumidified PEMFCs utilize the water produced internally to self-hydrate the membrane. An autohumidified system eliminates the need for a humidification system for water-reliant proton conductors. However, most experience with autohumidified operation has been disappointing.[3,4] Membrane hydration has only been maintained at low temperatures. Maintaining stable operation is difficult and the fuel cell must be hydrated to start up.

Buchi and Srinivasan[3] reported steady-state autohumidified operation in a standard fuel cell test cell with serpentine flow channels using hydrogen at 1 bar and air 1.7 bar for temperatures 60°C and below; at 70°C and above the polymer electrolyte dried out and the fuel cell stopped functioning. They suggested that at sufficiently low temperatures and currents the water produced at the cathode would diffuse to the anode and hydrate the membrane.

Recently, Hogarth and Benziger[5] demonstrated autohumidified operation with a hydrogen and oxygen PEMFC up to 115°C by increasing the operating pressure to 3 bar. They showed that the flow-channel design was critically important to autohumidified operation; a "stirred tank" design philosophy permitted autohumidified operation at higher flow rates and higher temperatures than the serpentine flow channel. Hogarth and Benziger derived criteria for autohumidified operation with both hydrogen/oxygen and hydrogen/air that showed the relationship between temperature, pressure, and feed stoichiometry for different types of flow fields.

These previous investigations of autohumidified fuel cells have been limited to steady-state operation. A greater understanding of the dynamic operation of an autohumidified PEMFC is required to characterize the operating regime of the cells and their response to a system disturbance. Key questions are (*i*) how to start up the autohumidified fuel cell, (*ii*) how the autohumidified fuel cell responds to changes in load, flow rates, temperature, and pressure; and (*iii*) under what conditions the fuel cell current will extinguish.

We recently developed the stirred tank reactor (STR) fuel cell to study the dynamic operation of PEMFCs.[6] The STR PEMFC is a one-dimensional differential cell; eliminating longitudinal gradients greatly simplifies the analysis of fuel cell operation. The STR differential element can also serve as a building block to predict performance for more complex fuel cell designs. We previously reported results with the STR PEMFC that demonstrate analogous phenomena between the water balance in a differential PEMFC and the energy balance in a classic exothermic stirred tank reactor.[7] The balance between water production and water removal in an autohumidified STR PEMFC leads to the existence of ignition/extinction of the fuel cell current and multiple steady states. These concepts are essential for understanding start-up and transient responses to changes in load, flow rate, and temperature in the autohumidified PEMFC.

The start-up and dynamic response of an autohumidified PEMFC is reported in this paper. We demonstrate that the current in a dry PEMFC can be "ignited" by direct water injection to initiate sustained autohumidified operation and characterize the ignition conditions. The ignition of the fuel cell depends on the temperature, flow rates, and external load resistance. Multiple steady states are manifested under conditions of fixed load and potentiostatic control of the load. Start-up and dynamic response times ranging from instantaneous to days are shown to depend on the rate of water accumulation in the polymer electrolyte membrane. We present basic design principles to size and operate autohumidified PEMFCs.

The paper is structured as follows. The STR PEMFC is described and time series data of autohumidified operation is presented for galvanostatic, potentiostatic, and constant load control. Data demonstrating current ignition and extinction are presented. The underlying physics behind steady-state multiplicity in an autohumidified PEMFC are described. The critical conditions for ignition and extinction of PEMFCs are presented and criteria for ignition by water injection are derived. We conclude with a discussion of design criteria for autohumidified PEMFCs.

Experimental

Experiments were conducted with custom-built STR fuel cells shown schematically in Fig. 1a; the active cell area was ~1.9 cm^2. The anode and cathode were diamond-shaped gas plenums machined from graphite with pillars to improve pressure uniformity on the membrane electrode assembly (MEA). The pillars and the outlets were all configured so that any liquid water at either the cathode or anode could freely drain by gravity. No liquid water would collect inside the fuel cell. The fuel cell was placed in an insulated temperature-controlled environment illustrated in Fig. 1b. Sensiron SHT75 (Sensiron AG, Switzerland) digital temperature and humidity sensors were placed directly in the outlet gas streams to record the exit relative humidity (RH) and temperature of the anode and

[z] E-mail: benziger@princeton.edu

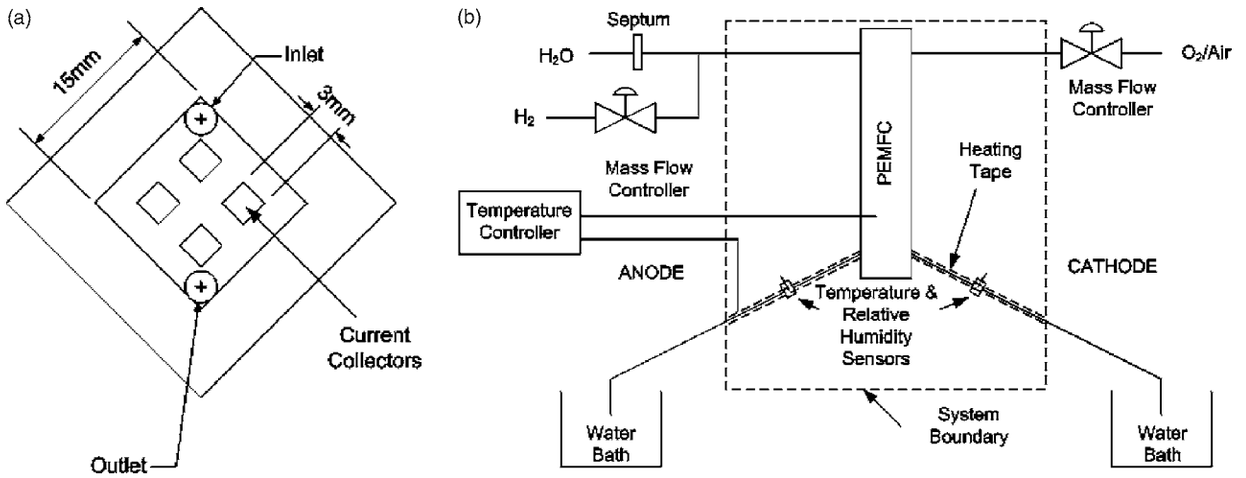

Figure 1. (a) Schematic of the flow channel plate for the STR fuel cell. The flow channel plate is an open plenum with four pillars to apply pressure to the MEA and act as current collectors. (b) Schematic of custom STR fuel cell test station. The flow channels are oriented to allow liquid water to freely drain by gravity from both the anode and cathode.

cathode. Because the fuel cell operated as a stirred tank reactor system, the RH in the effluent is approximately equal to the RH throughout the fuel cell.

Nafion/carbon-cloth MEAs were fabricated in our lab. Nafion 115 membranes (Ion Power, Inc., DE, USA) were cleaned by sequential boiling for 1 h in 3 wt % peroxide, deionized (DI) water, 1 M sulfuric acid, and DI water. The Nafion was pressed between A6 ELAT-type electrodes (E-TEK division of DeNora, NJ, USA) which contained 0.5 mg/cm^2 of Pt on carbon. The carbon paper was coated with 0.6 mg/cm^2 of 5 wt % Nafion solution to improve the 3-phase interface. MEAs were pressed at 140°C for 90 s at 40 MPa pressure before being placed into the cells. Four bolts on the cell were each tightened with 3 Nm of torque. The fuel cell circuit was completed by connecting the anode and cathode to an Arbin Instruments (TX, USA) potentiostat running MSTAT4+ software.

Experiments were conducted with dry feeds of hydrogen and oxygen with flow rates of 10 and 5 cm^3/min, respectively. All experiments were conducted with constant flow rates so that flow control dynamics were decoupled from reactor dynamics. The flow rates and fuel cell size were matched so the diffusive mixing in the gas space at the anode and cathode kept the compositions uniform. Pure oxygen was fed to the cathode to simplify the analysis of the experiments. We have demonstrated elsewhere that the results are readily extended to apply to dry hydrogen/air systems with an adjustment for nitrogen as a dilutent.[5,8]

To investigate the dynamic operation the fuel cell was equilibrated for a minimum of 1 h with a fixed load resistance or controlled by the Arbin potentiostat/galvanostat to maintain either a fixed voltage or current. After the system was at steady state, a step change was made to either the load resistance, voltage, or current and the response of the system was monitored. Rapid current–voltage (I–V) sweeps representing constant water content in the membrane were conducted by sweeping the voltage at 20 mV/s from 0.95 down to 0.2 V. The entire sweep took ~45 s. These rapid I–V sweeps were done before and at various intervals after the step change in load resistance, voltage, or current. The steady-state I–V curve was obtained by stepping the fuel cell through a series of current set point values from high current to low current and back to high current. At each set point the system was allowed to equilibrate for at least 1 h to allow the water content in the membrane to equilibrate. The step interval was smaller in the lower current range as this was where the greatest changes occurred. A current interrupt technique was used as an indication of the internal resistance of the MEA. A total of 10 pulses, 1 ms apart, at an amplitude of 40 mA were applied. The MSTAT4+ software was used to analyze the data.

Current ignition of dry fuel cells was conducted by injecting a known amount of water directly into the flow chamber at the anode with a syringe. A tee was placed at the anode inlet. The hydrogen was fed via the tee branch. A septum was placed in the inlet run where a syringe could be inserted into the anode gas space approximately 0.5 cm away from the gas diffusion layer (GDL).

The current densities reported here are lower than "state of the art" PEMFCs with humidified feeds.[9] We used a Nafion 115 membrane and made our own MEAs, which are inferior to commercial MEAs using Nafion 112. The phenomena presented here are general, but the quantitative details depend on specifics of the MEA. We show how the results presented here scale to other membrane systems and changing from pure O_2 to air at the cathode.

Results

Steady-state I–V curve and steady-state multiplicity.— Figure 2 shows both the steady state I–V curve produced from the current stepping program shown in Fig. 3 and a rapid-scan I–V curve swept in <45 s after equilibrating the membrane at 200 mV. Because the

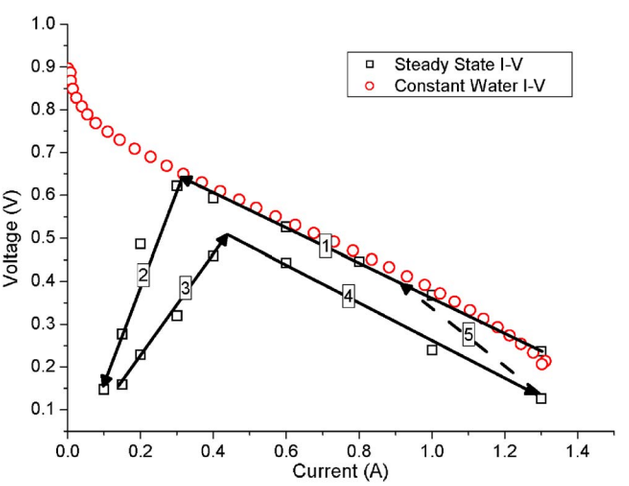

Figure 2. Rapid ("constant water content") and steady-state I–V curves of the STR fuel cell operating with dry feeds. The steady-state I–V curve was obtained after equilibrating the cell at a series of current set points as shown in Fig. 3.

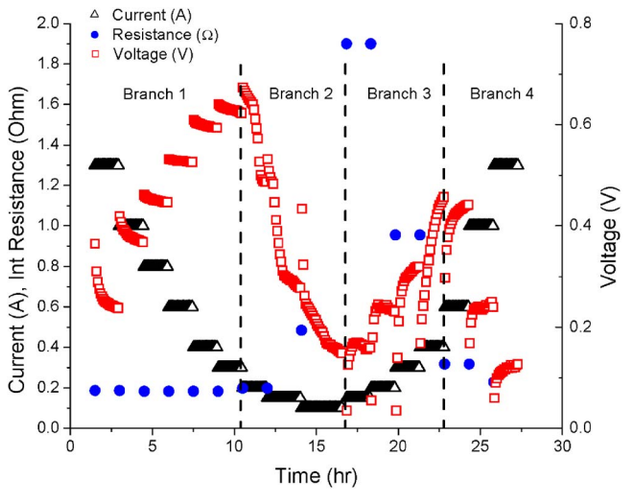

Figure 3. Time series data for the steady-state I–V curve swept in Fig. 2. The graph shows the current set point, voltage response of the system, and the internal resistance of the membrane. The different branches on the I–V curve are shown as separate regions in the time series data.

I–V curve is swept in a time period of <100 s, the water content in the membrane does not change significantly and hence the internal resistance of the MEA is nearly constant throughout; we refer to such rapid-scan I–V curves as "constant water content." The constant water I–V curve is similar in nature to the standard I–V curves reported in the literature obtained with humidified feeds. When the feed is humidified the membrane is fully hydrated and the water content in the membrane does not change as water is produced.[9]

The points on the steady-state I–V curve shown in Fig. 2 correspond to the equilibrated current and voltages shown in Fig. 3. The cell was initially equilibrated at 60°C with a current of 1.3 A. At this condition the water produced in the fuel cell greatly exceeds the maximum water that can be removed as water vapor. Maximum water vapor removal is equivalent to a current of only 0.36 A. The steady-state and constant water content I–V curves mirror each other as the current was reduced from 1.3 A to 0.3 A along branch 1. The internal MEA resistance was also constant, as shown by Fig. 3. The curves mirror each other because the water removed by convection remains lower than the total amount of water produced. Under such conditions the RH is at or close to 100%, which keeps the membrane fully hydrated. This was confirmed by RH measurements of both effluent streams. At 0.3 A and 0.65 V (load resistance of $\sim 2.2\ \Omega$) the steady-state I–V curve peaks; below 0.3 A the steady-state voltage decreases with each successive reduction in current. With each decrease in the current set point the voltage decreased, over time approaching a steady-state voltage. The concurrent decrease in current and voltage are shown along branch 2 of the steady-state I–V curve.

The internal resistance increased from 0.2 Ω when the current was 0.3 A to 1.8 Ω when the current was 0.1 A. The concurrent decrease in current and voltage along branch 2 falls on a ray from the origin of the I–V plot, indicating that the external load resistance was approximately constant while the internal MEA resistance was increasing. This suggests that there is a critical load resistance for autohumidified fuel cell operation. Along branch 2 of the steady-state I–V curve the RH at both the anode and cathode decreased with decreasing current. The RH was ~100% at a current of 0.3 A and decreased to ~30–40% at a current of 0.1 A. The steady-state RH at the anode was slightly lower than the RH at the cathode along branch 2; at a current of 0.1 A the cathode RH was 37% and the anode RH was 33%.

After equilibrating the cell at 0.1 A the current was increased stepwise. When the current was increased the voltage initially dropped, then increased, approaching a steady-state value, as shown in branch 3 on Fig. 3. The steady-state voltage increased with increasing current up to a current of ~0.4 A. The RH of the anode and cathode both increased from 35% at 0.1 A to ~100% at a current of 0.4 A. The internal MEA resistance also decreased from 1.8 to 0.4 Ω, indicating the membrane was being rehydrated. As the current was increased above 0.4 A the transient voltage response was the same, but the steady-state voltage decreased with increasing current. These data are shown along branch 4 in Fig. 2 and 3. The RH of the anode and cathode were both 100% for currents greater than 0.4 A. As shown in Fig. 2, the fuel cell did not recover to the original performance within the time period of the experiment. The voltages were consistently lower after the membrane had been dehydrated. Rehydration of the membrane was not reversible. The critical load resistance to dehydrate the membrane and extinguish the fuel cell current was ~2 Ω (the slope along branch 2), while the load resistance had to be reduced to ~1 Ω (the slope along branch 4) to rehydrate the membrane. In other experiments (not shown) where the fuel cell was shorted for an extended period of time (greater than 24 h) the system was able to regain its original performance as shown by branch 5 and the cycle would repeat.

The peak of the steady-state autohumidified I–V curve, where the membrane begins to dehydrate, shifts with temperature. For MEAs employed in the experiments reported here the critical load resistance to dehydrate the membrane was ~1.4 Ω at 80°C and ~3.2 Ω at 50°C. We observed that the critical load resistance for dehydrating the membrane varied depending on MEA preparation and potentially other factors, including age and compression force; however, the general shape of the curves and hysteresis illustrated in Fig. 2 were always apparent.

The dynamic voltage response of the autohumidified fuel cell system to step changes in current is shown in Fig. 3. The internal resistance of the cell was also recorded after steady state was achieved for each set point change. Steady state was assumed when the voltage of the system had changed by no more than 5% in a 30 min period. The dynamic response changes between low and moderate currents because of differences in membrane hydration. At moderate currents, >0.3 A, more water is produced by the cell than is removed by convection of water vapor; hence, the effluent streams and the membrane are fully hydrated. When the current is reduced below this critical point there is insufficient water produced to fully humidify the effluent streams, hence the RH in the flow channels drops and the membrane begins to dry. It is important to note that this critical point is dependant on the specific systems conditions such as temperature, flow rate, and pressure as defined elsewhere.[5]

Steady-state multiplicity – current, voltage, and resistance control.— Figure 2 demonstrates that PEMFCs that are autohumidified exhibit multiple steady states. Multiple steady states imply that for the same set of operating parameters—fuel cell temperature, pressure, feed flow rates, and current—there are two different possible steady-state voltages. Over the current range between 0 and 0.3 A in Fig. 2 the same operating parameters result in two different operational states; branches 2 and 3 show that two different steady-state voltages can be obtained at the same temperature, pressure, and flow rates. There are also two different voltages for the same current at above 0.4 A, where branches 1 and 4 show differences between before and after the membrane has been dehydrated.

The steady-state I–V curve presented in Fig. 2 was obtained by stepping the current set point and recording the voltage. The steady-state I–V curves were the same when obtained under potentiostatic control and with load control. Figure 4 shows the steady-state I–V data obtained from the three methods of control of an autohumidified PEMFC. All three I–V curves were obtained at the same temperature, pressure, and feed flow rates. For fuel cell operation only one of the three parameters—current, voltage, and load resistance—can be specified independently. Once any one of those parameters is specified, the other two are fixed. Figure 4 also indicates that for

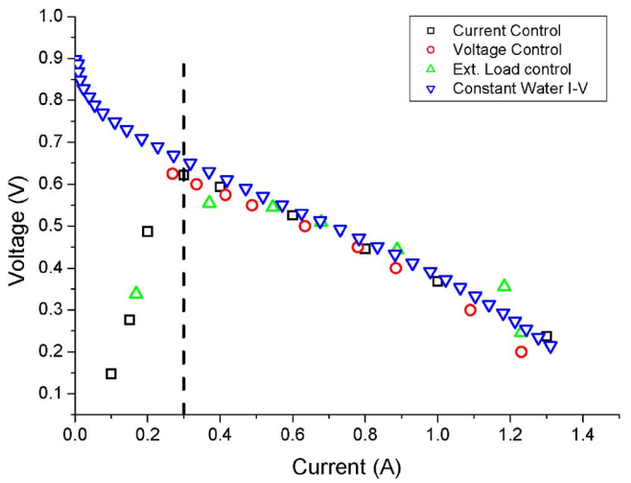

Figure 4. Steady-state I–V curve equilibrated at constant load, current, and potential and rapidly swept constant water I–V curve. To the right of the vertical line shown, stable fully autohumidified operation is achieved where the humidity at the anode and cathode are both 100%.

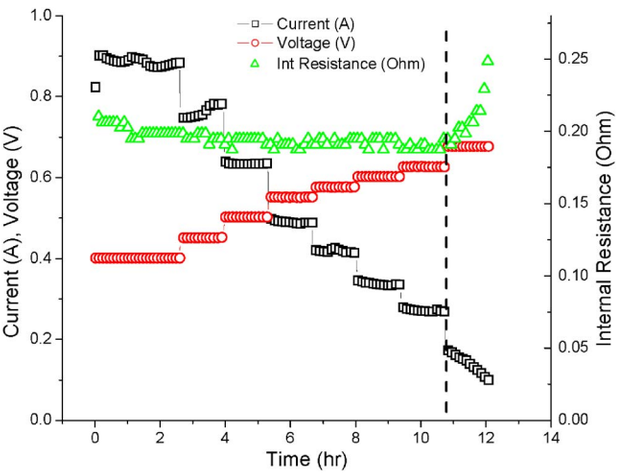

Figure 6. Dynamic response of the autohumidified STR fuel cell to changes in potential. The dashed vertical line shows the condition at which the membrane begins to dehydrate.

autohumidified PEMFC operation there is a critical load resistance for stable operation; the fuel cell system employed here had a critical load of ~2 Ω at the flow rates and the temperature specified. Operating the fuel cell with a load greater than 2 Ω would cause the membrane to eventually dehydrate and the fuel cell current would extinguish.

The dynamic response of the autohumidified STR PEMFC to changes in external load at 60°C and 1 atm is reported in Fig 5. This is analogous to Fig. 3, but now the external load was progressively stepped up from 0.3 Ω at intervals of 1.5 h. The voltage and current response were measured continuously while the internal resistance was measured at the end of each step. As shown in Fig. 5, the voltage and current respond immediately and remain almost constant for each load change up to 1.5 Ω. The internal resistance of the cell is also constant. Increasing the load resistance to 2.0 Ω causes the current and voltage to decrease with time, and after an hour the electronic load loses control. This directly supports the observations in Fig. 2 and 4. The internal resistance of the MEA also increases considerably when the load resistance is increased to 2 Ω, indicating the membrane is dehydrating. The loss of control is an artifact of the system due to controller dynamics, as we have demonstrated elsewhere.[10] When a 2 Ω resistor is used, the current and voltage fall to 0 smoothly.

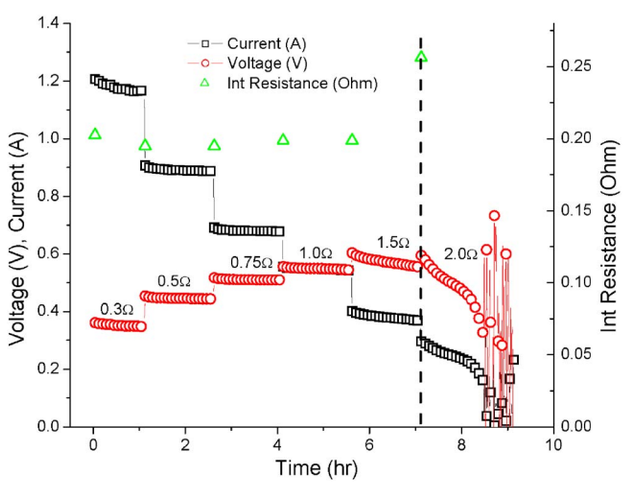

Figure 5. Dynamic response of the autohumidified STR fuel cell to changes in external load. The potentiostat was programmed to maintain a constant load. When the fuel cell current began to extinguish the potentiostat became unstable.

Figure 6 shows the dynamic response of the system to set point changes in potential. After equilibration at 200 mV for 24 h the potential was increased from 0.4 to 0.675 V. Below 0.625 V the operation is generally stable, as is the internal resistance. When the potential is increased to 0.675 V the current approaches 0 over time as it extinguishes and the internal resistance of the membrane increases rapidly. Again, this is consistent with the results for controlling the current or load resistance.

Ignition of a dry fuel cell.— As shown in Fig. 2 and 3, if the fuel cell is operated with too large a load resistance, the fuel cell is not capable of producing enough water to keep the membrane hydrated and current extinguishes. After extinction it is not possible to reignite the fuel cell current by simply changing the load resistance; even short-circuiting the fuel cell is not sufficient to start the fuel cell once the membrane dries out. Starting a PEMFC with a dry membrane requires some method of hydrating the membrane. With dry feeds one method of introducing the required water is through direct injection of liquid water at the anode.

Figure 7 shows the result of directly injecting 100 μL of water at the anode of an autohumidified STR PEMFC that had been extinguished. The cell current was extinguished by driving a 20 Ω external load, then the external load was changed to 0.2 Ω. Even with the 0.2 Ω resistor the cell current remained extinguished (<1 mA) for more than 60,000 s. Immediately after water injection the cell current ignited, rising to >400 mA within 100 s. Over a longer time period of days the performance continues to steadily increase before reaching steady state after 3 days.

This experiment was performed under a series of conditions (not shown). The cell always responded to the injection of water with an increase in current; however, ignition with a stable steady current was only obtained at proper conditions of sufficiently low temperature and load resistance. When the cell was injected with 100 μL of water at 80°C with an external load of 0.2 Ω, the current rapidly rose to 0.5 A but then decayed and the cell current extinguished within 1000 s. When injecting the cell with water at 60°C with an external load of 10 Ω, the current rose to 100 mA after 100 μL of water was injected and then decayed to near zero.

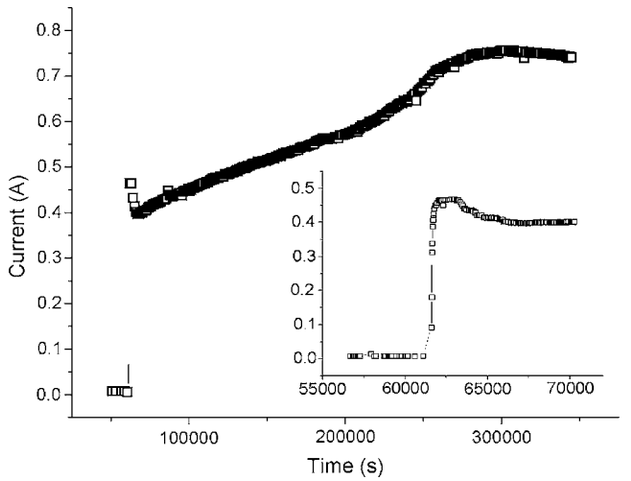

Figure 7. Ignition of an autohumidified fuel cell at 60°C after injecting 100 μL of water at the anode at 61,000 s. Prior to injection the fuel cell was extinguished and maintained at 60°C with dry feed for several hours before igniting.

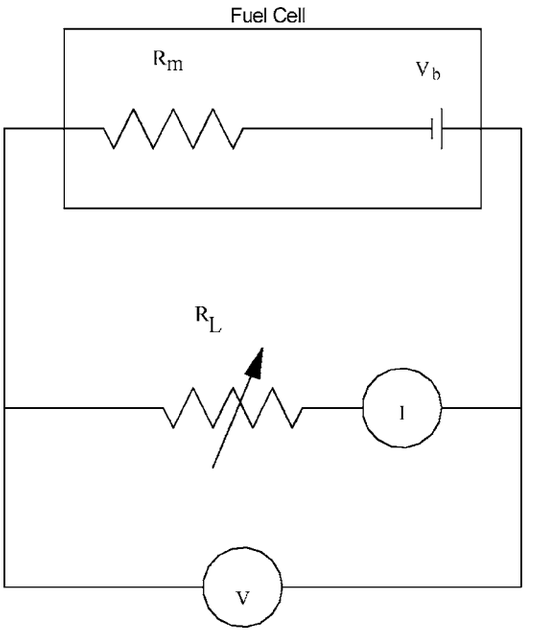

Figure 8. Simplified circuit model of a fuel cell.[14] I–V curves report the voltage across the load resistor as a function of the current through the load resistor. A galvanostat adjusts the load resistor to maintain the current through the load resistor constant while a potentiostat adjusts the load resistor to maintain the voltage across the load resistor constant.

Discussion

Steady-state multiplicity.— The steady-state I–V curves for the autohumidified PEMFC shown in Fig. 2 and 4 are different from the traditional I–V curve found in the literature. There is a maximum in the voltage at a finite current and the same voltage is obtained for two different currents. This unusual I–V curve results from the variable internal resistance of the polymer membrane as the hydration of the membrane changes in the autohumidified fuel cell. Most PEMFC studies have avoided the problem of variable water content by humidifying the feed, which keeps the membrane water content constant. Benziger and co-workers[11] have previously reported steady-state multiplicity of autohumidified PEMFCs with fixed load resistance. In addition to the work of Benziger and co-workers, Srinivasan and Buchi[3] and Watanabe and co-workers[12] have reported autohumidified PEMFC operation, but they did not examine the dynamic operation during startup and current extinction that are indicative of steady-state multiplicity. There are also recent reports in the literature where current oscillations occur when operating at reduced RH, which can also be explained by the presence of multiple steady states.[13]

Branches 2 and 3 in Fig. 2 reveal that two different voltages can be obtained at the same current when the current is below the level to fully humidify the effluent streams from the fuel cell. Figure 2 and 4 also illustrate that two different steady-state currents exist at the same voltage for the autohumidified PEMFC. According to Fig. 2, if the current was 0.3 A the steady-state voltage could be either 0.65 V (at the intersection of branches 1 and 2) or 0.35 V (along branch 3). Multiple voltages at the same current only occur when the load resistance is $<2\ \Omega$. One steady state is an extinguished current state where the membrane is dehydrated and current and voltage are near zero. The other steady state is an "ignited" state where the membrane is hydrated and the current is >0.3 A. If the load resistance is greater than the critical value of 2 Ω there is a single state, that being the extinguished state with the current and voltage both near zero.

Why does steady-state multiplicity occur with the autohumidified PEMFC? The membrane water content, and hence its resistance, is controlled by a balance between water produced by the current and the water removed by convective flow through the cell. To explain how the variable membrane resistance affects fuel cell performance, consider the simplified circuit model of the fuel cell shown in Fig. 8.[14] The fuel cell consists of a battery and a resistor series. The ideal battery voltage, V_b, represents the difference in chemical potential between the anode and cathode (Eq. 1). For an ideal system the chemical activities, a_i, are the partial pressures for hydrogen and oxygen and the water activity, a_w, is the ratio of the partial pressure of water to the vapor pressure of water at the fuel cell temperature

$$V_b = \frac{-\Delta G^0}{2F} - \frac{RT}{2F}\ln\left(\frac{a_{H_2}^{\text{anode}}(a_{O_2}^{\text{cathode}})^{1/2}}{a_w^{\text{cathode}}}\right) \quad [1]$$

The fuel cell resistor is the membrane resistance for proton transport. The membrane resistance depends on the physical dimensions of the membrane (thickness t and area A) and the resistivity of the polymer membrane, ρ_m. For Nafion membranes the resistivity as a function of water activity was measured by Yang et al.[15] and empirically fit by Eq. 2. For simplicity, we assume ideal electrodes so there is no activation overpotential and we also ignore mass-transfer limitations at high currents. Capacitive elements are not included because they only affect the time to reach steady state; they do not change the steady-state voltage or current in the fuel cell

$$R_m = \frac{t_m}{A_m}\rho_m = \frac{t_m}{A_m}[1 \times 10^7 \exp(-14a_{w,m}^{0.2})\Omega - cm] \quad [2]$$

The water inventory in the membrane is determined by a balance between water production in the fuel cell and water removed by convection of liquid water and water vapor. Water production is equal to half the current, which depends on the load resistance and the membrane resistance as given by Eq. 3

$$\text{water production} = \frac{i_{H^+}}{2} = \frac{V_b}{2(R_L + R_m)} \quad [3]$$

Water is removed as both liquid and vapor. When liquid water exits the STR fuel cell the water activity in the fuel cell is unity and the membrane is fully hydrated and its resistance is a minimum, $R_{m,\min}(R_{m,\min} = 8^{t_m}/A_m\Omega)$. The rate of water vapor removal is equal to the total molar flow exiting the fuel cell at the anode and cathode, F_A and F_C, multiplied by the mole fraction of water in the vapor, $x_w^A = P_w^A/P_T$, $x_w^C = P_w^C/P_T$

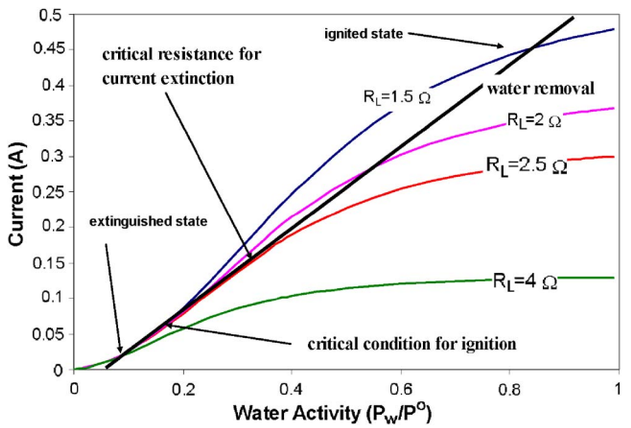

Figure 9. The water balance for an autohumidified PEMFC. The water production curves are shown for several different load resistances; they are based on a Nafion 115 membrane with resistivity given by Eq. 2. The water removal line is for a flow rate of 10 cm^3/min H_2 at the anode and 5 cm^3/min O_2 at the cathode at 1 bar and 60°C. Both ignited and extinguished steady-state currents are highlighted. The critical load resistances for extinction and ignition where the water removal line is tangent to the water production curves are also shown.

$$\begin{pmatrix}\text{water vapor removed}\\ \text{by convection}\end{pmatrix} = (F_A x_w^A + F_C x_w^C) = (F_A P_w^A/P_T + F_C P_w^C/P_T) \quad [4]$$

The maximum amount of water that can be removed as a vapor is when the partial pressure is equal to the saturation vapor pressure, P_w^o. When the rate of water production is less than the maximum rate of water vapor removal the water activity in the membrane is less than one and the membrane resistance is greater than the minimum resistance obtained with fully hydrated membranes.

At steady state water production must be balanced with water removal as expressed in Eq. 5, where F is Faraday's constant

$$\text{(water produced)} = \text{(water removed)}$$

$$0.5\frac{V_b}{R_L + R_m} = F\left\{F_A a_w^{\text{anode}}\frac{P_w^A}{P_T} + F_C a_w^{\text{cathode}}\frac{P_w^C}{P_T}\right\} \quad [5]$$

For simplicity we assume that the water activity in the gas effluents at the anode and cathode are in equilibrium with the water activity in the membrane. More complex models can be employed to account for mass-transfer limitations, finite reaction kinetics, etc., but those details are not necessary to understand the basic physics of steady-state multiplicity in the autohumidified PEMFC.

The steady-state water balance is illustrated in Fig. 9. Water produced for different fixed-load resistances (left side of Eq. 5) and water removed (right side of Eq. 5) are plotted as functions of the water activity in the membrane. The water produced is a sigmodial curve. At low water activity the membrane resistance is high and the current is small because the overall current is limited by the membrane resistance to proton transport. As the water activity increases the membrane resistance decreases exponentially, giving rise to the rapid rise in the current. As water activity approaches unity the membrane becomes hydrated, its resistance approaches its minimum value, and the current approaches a limiting value of $I_{\max} = V_b/(R_L + R_{m,\min})$. For the Nafion 115 membrane in the 1.9 cm^2 cell the minimum resistance is $R_{m,\min} \approx 0.05\ \Omega$ (assuming no membrane/electrode interfacial resistance).

Water removal is approximately a straight line (neglecting the small change in molar flow rate due to hydrogen and oxygen reacting). The water removal line shown has a negative intercept because in our experiment the fuel cell effluent goes into a water bath, resulting in back diffusion of water. This is equivalent to having a small amount of water in the feed streams; we estimated the back diffusion of water to correspond to the equivalent of a current density of 20 mA. The intersection of the water production curve and the water removal line corresponds to the steady state. At low to moderate load resistances ($R_L = 1.5\ \Omega$ in Fig. 9) the water production curve intersects the water removal line at three points. At high water activity there is a significant current, and this corresponds to an ignited state of the fuel cell. This state corresponds to autohumidified operation. There is also an intersection near the origin where the current is extinguished. This is the dehydrated fuel cell. There is also a third intersection at low water activity ($a_w \sim 0.25$ on the $R_L = 1.5\ \Omega$ curve) where the water production curve is beginning its exponential rise. This state is inherently unstable. For water activity greater than $a_w = 0.25$ the water production exceeds water removal, so the fuel cell hydrates and approaches the ignited state. When the water activity is less than $a_w = 0.25$ the water removal is greater than water production, so the full cell membrane dehydrates and the fuel cell current extinguishes.

Changing the load resistance causes the water production curve to shift up for lower loads and down for higher loads. It is easy to see that above a critical load resistance of 2.5 Ω the water production curve lies completely below the water removal line, corresponding to the critical resistance identified in Fig. 2 and 4, where the autohumidified fuel cell dehydrates. It is impossible to have sustained operation of an autohumidified PEMFC when the load resistance increases above this critical value.

Sweeping an I–V curve for the fuel cell involves altering the load resistance, R_L, between 0 (short circuit) and ∞ (open circuit) and measuring the current through (I) and the voltage across (V) the load resistor. Under voltage or current control the potentiostat or galvanostat varies the load resistor to try to maintain the set point voltage or current. It is impossible for the autohumidified fuel cell to be controlled if the controller (galvanostat or potentiostat) needs to maintain the manipulated load resistance at a value greater than the critical value for extinction. This is why branch 2 of the steady-state I–V curve falls along a ray from the origin corresponding to the critical load resistance.

Ignition/extinction hysteresis.— Figure 2 illustrates that autohumidified PEMFCs do not operate reversibly. When the load exceeds the critical load resistance and the fuel cell extinguishes, it requires a lower load resistance to reignite. Figure 2 also shows that after reignition and liquid water is present the fuel cell may not fully recover for a very long period of time.

The hysteresis between ignition (branch 3, Fig. 2) and extinction (branch 2, Fig. 2) of the autohumidified fuel cell can be explained with reference to water balance, shown in Fig. 9. The ignited current state is the intersection of the water production curve and the water removal line. At a load resistance of 1.5 Ω the steady-state current is 0.45 A and the membrane water activity is 0.88. Increasing the load resistance to 2 Ω causes the steady-state current to decrease to 0.3 A and the membrane water activity in the membrane decreases to 0.55. When the load resistance is increased to 2.5 Ω the water removal line is tangent to the water production curve at a water activity of 0.35. This corresponds to the critical resistance for extinction. The water production curve has negative curvature at the point of tangency and any further increase in load resistance causes the entire water production curve to the right of the extinguished steady state to fall below the water removal line so there is no longer an ignited steady state. If the fuel cell starts from an extinguished state, shown on Fig. 9, ignition does not occur until the load resistance is decreased to the point that the water production curve becomes tangent to the water removal line at the point where the water production curve has positive curvature, so any decrease in the load resistance results in the water production curve being above the water removal line to the right of the tangent point.

Figure 10 is an enlargement of Fig. 9 to illustrate that the ignition requires a lower external load resistance (and hence higher fuel cell

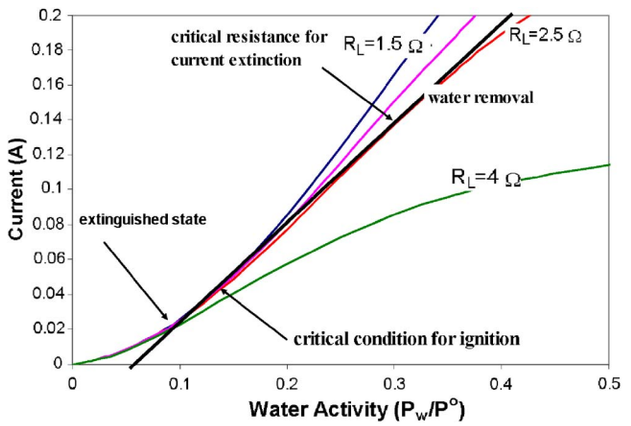

Figure 10. Enlargement of the water production and water removal curves for an autohumidified PEMFC. The critical load resistances for extinction and ignition are where the water removal line is tangent to the water production curves.

current) than extinction of the fuel cell current. This hysteresis between extinction and ignition is shown experimentally in Fig. 2. The fuel cell current extinguished at a load resistance of ~2.2 Ω, but the load resistance needed to be reduced to ~1 Ω to reignite the fuel cell current.

There is a second hysteresis evident in Fig. 2 between the ignited state before (branch 1) and after (branch 4) the fuel cell current was extinguished. In the fully humidified region (currents greater than 0.45 A) the voltages obtained at the same current were greater before the fuel cell had been extinguished than after extinguishing the current. We believe this hysteresis is the result of changes in the membrane/electrode contact. Nafion membranes swell and shrink as they absorb and desorb water. We suggest that the dynamics of swelling and shrinking are not reversible on moderate time scales. This is evident in Fig. 7. After the fuel cell was ignited the current rose relatively quickly in ~100 s, and on the time scale of 5000 s (~1 h) the current was nearly constant. However, when viewed on the longer time scale of 100,000 s (~1 day) there was a significant increase in the fuel cell current and it took more than 2–3 days for the fuel cell current to fully stabilize. This result indicates are long time process involved with equilibrating PEMFC membranes so that on moderate time scales of hours there may be substantial hysteresis associated with water sorption and the membrane/electrode interface. Previous studies have reported long-time dynamic responses to changes in load and temperature that were attributed to membrane swelling altering the membrane/electrode contact.[16]

Fuel cell ignition.— A few papers have reported PEMFC autohumidification operation, but those authors did not identify an ignition condition or multiple steady states.[3,4] In those studies the fuel cell was switched from a humidified feed to a dry feed, and the sustained operation was observed at temperatures below 60°C [3] and 80°C.[14] If it is necessary to have a humidified feed to start up the fuel cell, the benefits of operating autohumidified with dry feeds are defeated. The unstable steady state identified in Fig. 9 is the critical condition to the start-up of an autohumidified PEMFC. If the water activity in the membrane can be increased above the critical value then the fuel cell will ignite. Direct injection of sufficient water to raise the water activity above the critical value can then ignite the fuel cell current.

When water is injected into the anode of the fuel cell, some of the water is absorbed into the membrane, while some of the water is carried out in effluent from the fuel cell. We can estimate the critical amount of water that should be injected to ignite the fuel cell as follows. The critical membrane water activity for ignition is ~0.35, which corresponds to a water content of ~4 water molecules per SO_3^-.[15,17,18] It takes the water about 100 s to absorb into the polymer membrane.[18,19] Some water is also lost by liquid water draining from the anode. The amount of water injected to the anode less the amount of water vapor carried out in the anode effluent in 100 s less the amount of liquid water that drains from the anode should be equal to the water required to titrate the sulfonic acid groups to greater than $\lambda = 4H_2O/SO_3$. The required water injection for ignition of an autohumidified STR PEMFC is summarized in Eq. 6

$$\begin{aligned}(\text{water injection}) &> 4(\text{number of sulfonic acid groups}) \\ &\quad + \begin{pmatrix}\text{water vapor convection} \\ \text{in 100 s}\end{pmatrix} \\ &> \left[4\frac{(\rho_{\text{nafion}})(A_m)(t_m)}{(EW)} + F_A\frac{P_w^o}{P_T}(100\ s)\right] \quad [6]\end{aligned}$$

For a 2 cm^2 Nafion115 membrane at 60°C the required water injection based on Eq. 6 is 65 μL. Increasing the temperature to 80°C increases the required water injection for ignition to 120 μL. This prediction is in reasonable agreement with the experimental results that 100 μL was sufficient to ignite the fuel cell at 60°C but insufficient to ignite the fuel cell at 80°C. Ignition also requires that the load resistance be less than the critical value for autohumidified operation. It is impossible to ignite the PEMFC at 60°C if the load resistance is greater than 2.5 Ω.

Equation 6 shows several key features of the water injection requirement: (*i*) it decreases with membrane thickness (a 112 membrane would require less water to ignite than a 115 membrane), (*ii*) it increases with increased flow rate at the anode, (*iii*) it decreases with increased total pressure, and (*iv*) it increases with temperature.

Equation 6 is semiempirical, but it does provide simple useful design criteria for operation of autohumidified PEMFCs.

Implications for fuel cell design.— The STR PEMFC is not optimal for fuel cell performance, but it is useful to decouple spatial and temporal phenomena and provide guidance for design and control. Serpentine and other flow channel designs for fuel cells can be analyzed as a series of stirred tank reactors. The results presented here are generic for PEMFCs. Steady-state multiplicity and current ignition/extinction occur for any PEMFC operated with underhumidified feeds.

Fuel cells should operate at high efficiency and the current should not extinguish. Results presented here demonstrate that for autohumidified PEMFCs there exists a maximum load resistance that could be powered by a fuel cell without current extinction. Equation 7 presents the relationship between the sum of the load resistance and membrane resistance to the battery voltage (Eq. 1), the total molar feed flow rate at the anode and cathode, the total pressure, and the vapor pressure at the temperature of the STR PEMFC. Equation 7 is a conservative estimate that assumes the critical condition for extinction is water activity of unity. It is applicable to both H_2/O_2 and H_2/air fuel cells

$$R_{m,\min} + R_L < \frac{V_b(1 + P_w^o/P_T)}{2F(F_A + F_C)P_w^o/P_T} \quad [7]$$

If an operating temperature and pressure and fuel cell size are specified (fixing P_w^o, P_T, and $R_{m,\min}$), Eq. 7 relates the maximum load resistance to the feed flow rates to the fuel cell. Alternatively, if one specifies the temperature and pressure and the load resistance, Eq. 7 relates the fuel cell size and feed flow rates that are possible for stable operation. If the power requirement that the fuel cell must deliver to the load is also specified, Eq. 7 and 8 completely specify the size of the fuel cell and the feed flow rates

$$\text{Useful Power} = \left(\frac{V_b}{R_m + R_L}\right)^2 R_L \quad [8]$$

For more general flow channel designs Eq. 7 and 8 need to be integrated along the length of the flow channel. With flow channels,

ignition/extinction occurs locally, followed by front propagation along the length of the flow channels.[20]

A second important implication of the maximum load resistance for autohumidified operation concerns the use of shunt resistors or governors to control the power delivered to the load impedance. Once a load is attached to a fuel cell the current through, voltage across, and power dissipated in the load are all fixed. To vary any of those system variables it is necessary to add a variable shunt resistor in series with or in parallel to the load impedance. With autohumidified fuel cell operation the shunt resistance should be placed in parallel to the load impedance. Any reduction in current through the load is thus accompanied by a decrease in the total external resistance. The total internal current in the fuel cell, and hence the water production, is always maintained at a sufficient level to keep the membrane hydrated and the fuel cell does not extinguish. If a series shunt resistor were used to reduce the current in the load, the internal current in the fuel cell is decreased and the water production can decrease below the necessary level to keep the membrane hydrated.

Conclusions

The balance between water production and water removal is coupled with the membrane's resistance, resulting in a positive feedback that leads to multiple steady states in autohumidified PEMFCs. Multiple steady states exist where the same set of operating parameters—feed flow rates, temperature, pressure, and load resistance—can produce different operating states of voltage and current. These steady states correspond to different levels of water absorbed in the polymer membrane. A low membrane water content results in a low current or extinguished state. A high membrane water content results in a high current or ignited state. We demonstrated ignited and extinguished steady states where two different steady-state voltages are observed for the same temperature, pressure, feed flow rates, and current. We also showed steady-state multiplicity where two different currents can be obtained at the same voltage or the same load resistance. The steady-state multiplicity corresponds to different amounts of water in the polymer membrane.

The start-up and dynamic operation of autohumidified PEMFCs was demonstrated. For given feed flow rates, temperature, and pressure, there is a maximum load resistance that can be driven by the fuel cell where ignited operation is sustained. Higher load resistances cause the fuel cell current to extinguish. Criteria for scaling the load resistance as functions of the fuel cell operating parameters of flow rate, temperature, and pressure were developed for sizing and operating an autohumidified PEMFC.

The autohumidified PEMFC current can be ignited by direct injection of water. Criteria were derived for the water injection required to ignite the fuel cell current; the fuel cell current can only be sustained when the load resistance is less than the critical load resistance for extinction.

Acknowledgments

We thank the National Science Foundation (CTS -0354279 and DMR-0213707) for support of this work. W.H. thanks the Australian-American Fullbright commission for financial support.

Princeton University assisted in meeting the production costs of this article.

List of Symbols

A_m	area of membrane (cm^2)
a_i	thermodynamic activity of species i
EW	equivalent weight (g polymer/mole SO^3H)
F_A	molar flow at the anode (mol/s)
F_C	molar flow at the cathode (mol/s)
F	Faraday's constant (96,485 coul/mol)
ΔG	free energy across the fuel cell (J/mol)
i	current through the external load (A)
P_w	partial pressure of water (bar)
P_w^o	vapor pressure of water at fuel cell temperature (bar)
P_T	total gas pressure in the fuel cell
R	gas constant (82.05 cm^3-bar/mol-K)
R_m	membrane resisistance (Ω)
R_L	load resistance (Ω)
t_m	thickness of membrane (cm)
T	fuel cell temperature (K)
V	voltage drop across external load (V)
V_b	thermodynamic voltage of the fuel cell (V)
x_w	mole fraction water
ρ_m	resistivity of polymer membrane (Ω – cm)
ρ_{nafion}	density of nafion

References

1. A. Martin, in *Ninth Grove Fuel Cell Symposium*, Elsevier, London, U.K. (2005).
2. M. Fronk, in *Ninth Grove Fuel Cell Symposium*, Elsevier, London, U.K. (2005).
3. F. N. Buchi and S. Srinivasan, *J. Electrochem. Soc.*, **144**, 2767 (1997).
4. M. V. Williams, H. R. Kunz, and J. M. Fenton, *J. Power Sources*, **135**, 122 (2004).
5. W. H. J. Hogarth and J. B. Benziger, *J. Power Sources*, In press.
6. J. B. Benziger, E. Chia, E. Karnas, J. Moxley, C. Teuscher, and I. G. Kevrekidis, *AIChE J.*, **50**, 1889 (2004).
7. E. Chia, J. Benziger, and I. G. Kevrekidis, *AIChE J.*, **50**, 2320 (2004).
8. W. H. J. Hogarth, A. Hakenjos, and J. Steiner, *J. Power Sources*, Submitted (2006).
9. W. Vielstich, A. Lamb, and H. Gasteiger, Editors, *Handbook of Fuel Cells*, Vol. 1, Wiley, Indianapolis, IN (2003).
10. W. H. J. Hogarth, J. P. Nehlsen, and J. B. Benziger, *AIChE J.*, Submitted (2005).
11. J. F. Moxley, S. Tulyani, and J. B. Benziger, *Chem. Eng. Sci.*, **58**, 4705 (2003).
12. M. Watanabe, H. Uchilda, Y. Seki, M. Emori, and P. Stonehart, *J. Electrochem. Soc.*, **143**, 3847 (1996).
13. J. R. Atkins, S. C. Savett, and S. E. Creager, *J. Power Sources*, **128**, 201 (2004).
14. J. B. Benziger, M. B. Satterfield, W. H. J. Hogarth, J. P. Nehlsen, and I. G. Kevrekidis, *J. Power Sources*, **155**, 272 (2005).
15. C. Yang, S. Srinivasan, A. B. Bocarsly, S. Tulyani, and J. B. Benziger, *J. Membr. Sci.*, **237**, 145 (2004).
16. J. Benziger, E. Chia, J. F. Moxley, and I. G. Kevrekidis, *Chem. Eng. Sci.*, **60**, 1743 (2005).
17. T. Thampan, S. Malhotra, J. X. Zhang, and R. Datta, *Catal. Today*, **67**, 15 (2001).
18. D. R. Morris and X. D. Sun, *J. Appl. Polym. Sci.*, **50**, 1445 (1993).
19. M. B. Satterfield, P. W. Majsztrik, H. Ota, J. B. Benziger, and A. B. Bocarsly, *J. Poly. Sci. B*, **44**, 2327 (2006).
20. J. B. Benziger, J. E. Chia, and I. G. Kevrekidis, *Phys. Rev. Lett.*, Submitted (2006).